nature immunology

ARTICLES

https://doi.org/10.1038/s41590-019-0571-2

Programmed 'disarming' of the neutrophil proteome reduces the magnitude of inflammation

Jose M. Adrover[1], Alejandra Aroca-Crevillén[1], Georgiana Crainiciuc[1], Fernando Ostos[2], Yeny Rojas-Vega[3], Andrea Rubio-Ponce[1], Catia Cilloniz[4], Elena Bonzón-Kulichenko[5,6], Enrique Calvo[5,6], Daniel Rico[7], María A. Moro[2], Christian Weber[8,9,10], Ignacio Lizasoaín[2], Antoni Torres[4], Jesús Ruiz-Cabello[3,11,12,13,14], Jesús Vázquez[5,6] and Andrés Hidalgo[1,8*]

The antimicrobial functions of neutrophils are facilitated by a defensive armamentarium of proteins stored in granules, and by the formation of neutrophil extracellular traps (NETs). However, the toxic nature of these structures poses a threat to highly vascularized tissues, such as the lungs. Here, we identified a cell-intrinsic program that modified the neutrophil proteome in the circulation and caused the progressive loss of granule content and reduction of the NET-forming capacity. This program was driven by the receptor CXCR2 and by regulators of circadian cycles. As a consequence, lungs were protected from inflammatory injury at times of day or in mouse mutants in which granule content was low. Changes in the proteome, granule content and NET formation also occurred in human neutrophils, and correlated with the incidence and severity of respiratory distress in pneumonia patients. Our findings unveil a 'disarming' strategy of neutrophils that depletes protein stores to reduce the magnitude of inflammation.

Neutrophils are endowed with highly specialized features to combat infections. They accumulate receptors, proteases, antimicrobial peptides and proteins inside cytoplasmic granules that mediate the production of reactive oxygen species or DNA-based extracellular traps (NETs), both of which are highly toxic and allow for effective containment of pathogens[1,2]. Several types of granules coexist in the neutrophil cytoplasm[3], including primary (azurophilic) granules that store myeloperoxidase (MPO), secondary (specific) and tertiary (gelatinase) granules and secretory vesicles, each of which carry distinct types of cargo[1,4]. The different granules form at different stages of granulopoiesis in the bone marrow[5,6], and the synthesis of granule proteins declines as neutrophils differentiate[7,8]. In contrast, receptors needed for sensing, migration and phagocytosis are mostly synthesized once they reach the circulation[7,8].

After only 6–10 h in the circulation[9], neutrophils rapidly disappear from blood[10,11]. However, this does not imply immediate elimination, as they can be found within the vessels or parenchyma of multiple organs, with a preference for the spleen, bone marrow and lungs[10]. The homeostatic infiltration of granule-laden neutrophils, a process enabled by a cell-intrinsic program that relies on the chemokine receptor CXCR2 and the core clock protein Bmal1 (ref. [12]), can be potentially damaging to highly vascularized tissues such as the lungs. Indeed, lungs are highly susceptible to neutrophil-mediated damage, which can cause respiratory dysfunction and death, as shown in murine models of lung injury[13–15]. In humans, neutrophil-mediated acute vascular damage followed by pulmonary edema and distress is common in patients with underlying pneumococcal infections or other pre-existing conditions[13,16].

Here, we investigated whether specific mechanisms prevent neutrophil-inflicted toxicity in tissues. We found that the neutrophil proteome spontaneously 'disarms' as the neutrophils lose granule content during their lifetime in circulation. This resulted in a blunted capacity to produce NETs, rendering the neutrophils less toxic before they reached tissues, and protected the lungs from injury both in mice and in patients with pneumonia.

Results

The neutrophil proteome changes during the day. Neutrophils undergo transcriptional changes while in the circulation[12]. However, because transcriptional changes take a relatively long time (in the range of hours) and diurnal transcriptional programs in mouse neutrophils favor their migration into tissues, we examined alternative mechanisms that might protect the tissues from the toxic activity of neutrophils. We undertook a proteomic approach to explore the changes in protein content in neutrophils at different times after their release from the bone marrow. Because the number of neutrophils that can be purified from the blood of naïve mice at night (when neutrophils are released from the bone marrow) or at noon (when neutrophils have spent several hours in the circulation)[17] is low, we increased the number of night-like neutrophils released from the bone marrow by a one-time intraperitoneal injection at

[1]Area of Cell and Developmental Biology, Fundación Centro Nacional de Investigaciones Cardiovasculares, Madrid, Spain. [2]Unidad de Investigación Neurovascular, Department of Pharmacology, Faculty of Medicine, Universidad Complutense and Instituto de Investigación Hospital 12 de Octubre (i+12), Madrid, Spain. [3]Advanced Imaging Unit, Fundación Centro Nacional de Investigaciones Cardiovasculares, Madrid, Spain. [4]Department of Pneumology, Institut Clinic de Respiratori, Hospital Clinic of Barcelona, and Institut d'Investigacions Biomèdiques August Pi i Sunyer, University of Barcelona, Ciber de Enfermedades, Barcelona, Spain. [5]Cardiovascular Proteomics Laboratory, Centro Nacional de Investigaciones Cardiovasculares Carlos III, Madrid, Spain. [6]Centro de Investigación Biomédica en Red de Enfermedades Cardiovasculares, Madrid, Spain. [7]Institute of Cellular Medicine, Newcastle University, Newcastle upon Tyne, UK. [8]Institute for Cardiovascular Prevention, Ludwig-Maximillians University, Munich, Germany. [9]German Cardiovascular Research Centre (DZHK), partner site Munich Heart Alliance, Munich, Germany. [10]Department of Biochemistry, Cardiovascular Research Institute Maastricht, Maastricht, the Netherlands. [11]CIC biomaGUNE, Donostia-San Sebastián, Spain. [12]Ikerbasque, Basque Foundation for Science, Bilbao, Spain. [13]Ciber de Enfermedades Respiratorias, Madrid, Spain. [14]Universidad Complutense Madrid, Madrid, Spain. *e-mail: ahidalgo@cnic.es

zeitgeber time 4 (ZT4, or 4 h after lights on) of AMD3100, an antagonist for CXCR4 that induces the rapid mobilization of neutrophils from the bone marrow[18]. To increase the number of day-like neutrophils in circulation we injected blocking antibodies against endothelial selectins (1 mg kg^{-1}, intravenously at ZT5 at days −5, −3 and −1 before collection)[12,17] (Extended Data Fig. 1a). The proteomic analysis of these night- and day-like neutrophils isolated at ZT5 from the blood of wild-type mice yielded 6,677 proteins (Supplementary Table 1). A total of 171 proteins were differentially detected when comparing the night-like versus the day-like group, with proteins involved in regulation of the cytoskeleton (Arghdib, Rufy3), adhesion (Thbs1, Itgam), inflammasome (Nlrp3, Nlrp4e) and vesicular transport (Vps33b) (Fig. 1a) enriched in night-like neutrophils compared to day-like neutrophils. The differential expression of identified proteins in night- versus day-like neutrophils, such as VEGFR1, CD74, CD16/32, CD63 or CD14, was confirmed by flow cytometry (Extended Data Fig. 1b). Gene ontology analyses (Supplementary Table 2) indicated involvement of the differentially expressed proteins in immune defense, cytokine signaling and angiogenesis (Extended Data Fig. 1c). Night-like neutrophils were enriched for pathways linked to c-Kit signaling and platelet production, possibly reminiscent of their time in the bone marrow, as well as GTPase Rho signaling (Fig. 1b), consistent with the enhanced migratory capacity of 'younger' neutrophils[12]. Day-like neutrophils showed upregulation of protein synthesis, pathogen sensing and respiration (Fig. 1b), suggesting specialization for effector functions and enhanced TLR signaling, as previously suggested[12,19]. Comparison of the neutrophil proteome with transcriptional datasets associated with diurnal time[12] showed poor correlation (Extended Data Fig. 1d), suggesting that the proteomic changes are not driven by direct transcriptional regulation. These results therefore identify prominent changes in the neutrophil proteome that are associated with the time spent in the circulation.

Circulating neutrophils degranulate in the steady state. Based on the proteomic data, proteins stored in the various types of granules (azurophilic, specific and tertiary/gelatinase granules) were enriched in night-like neutrophils compared to day-like neutrophils (Fig. 1c and Supplementary Table 3). Enrichment in granule proteins was also detected in the proteome of circulating neutrophils from AMD3100-mobilized mice compared to daytime neutrophils (Extended Data Fig. 1e,f and Supplementary Table 4). Further analysis in the reactome database indicated that proteins differentially detected in the night- versus day-like neutrophils were associated with degranulation (Extended Data Fig. 2a), altogether suggesting a progressive loss of granules as neutrophils circulated.

Cytometric analysis of wild-type circulating neutrophils purified every 4 h (ZT1, ZT5, ZT9 (daytime); ZT13, ZT17, ZT21 (nighttime)) revealed circadian oscillations of side-scatter properties (Extended Data Fig. 2b), a feature that reflects cell granularity. To assess if these variations in side scatter were caused by degranulation, we stained cytospins of Ly6G$^+$ blood neutrophils purified at the same times as for MPO, a protein of azurophilic granules, and analyzed granule content by high-resolution confocal microscopy (Fig. 1d). The maximal abundance of MPO$^+$ granules was observed at ZT17 (midnight, when neutrophils leave the marrow), while the valley was at ZT1 (Fig. 1e and Extended Data Fig. 2c), indicating progressive loss of primary granules. MPO$^+$ granule content in neutrophils was in antiphase with elastase activity in plasma (Fig. 1f), suggesting the release of granule content into blood. A 12-h shift in the animal light cycle for three weeks completely readjusted the pattern of granule content in neutrophils (Extended Data Fig. 2d), indicating that degranulation was circadian in nature. Finally, Ly6G$^+$ neutrophils from lungs, spleen and liver had a lower MPO$^+$ granule content compared to Ly6G$^+$ neutrophils in the blood (Extended Data Fig. 2e,f). Thus, neutrophils undergo homeostatic degranulation in the circulation before they enter tissues.

Neutrophils progressively lose NET-forming capacity. Proteases stored in the azurophilic granules degrade the nuclear histones and promote chromatin decondensation during NET formation[20] and granule proteins have been identified in the NET proteome[21]. Among the proteins found in the proteomic analyses, those associated with NETs (Supplementary table 3) were enriched in the proteome of night-like neutrophils (Fig. 2a), suggesting that NET release is more prevalent at this time. To directly examine whether the formation of NETs varied during the course of a day, we treated Ly6G$^+$ neutrophils purified at ZT5 or ZT13 from the blood of wild-type mice with phorbol myristate acetate (PMA), a NET-inducing compound, and analyzed for the presence of extracellular DNA decorated with MPO protein and citrullinated histone 3 (cit-H3). We found that neutrophils at ZT13 (night) formed more NETs than at ZT5 (daytime) (Fig. 2b), revealing a correlation between diurnal azurophilic granule content and NET-forming capacity in blood Ly6G$^+$ neutrophils. Next, we assessed the presence of NETs by whole-mount immunostaining with the same markers in cremaster muscles of wild-type and Lyz2^{Cre}Mcl1$^{fl/fl}$ mice, which are neutropenic[22], after ischemia-reperfusion. Many more NETs were detectable in the muscles of mice at ZT13 than at ZT5, while no NETs were detected in the Lyz2^{Cre}Mcl1$^{fl/fl}$ mice (Fig. 2c). Thus, proteomic changes and degranulation of circulating neutrophils temporally coincide with loss of NET-forming ability.

Proteome changes are driven by CXCR2 and Bmal1. Diurnal changes in neutrophil transcription and migration are controlled by a cell-intrinsic mechanism, in which the expression of the chemokine *Cxcl2* is regulated by the molecular clock protein Bmal1 and leads to the cell-autonomous, diurnal activation of neutrophils by signaling through CXCR2 (ref. [12]). We therefore tested whether this mechanism caused the proteome changes. Treatment with CXCL2 induced degranulation in isolated wild-type Ly6G$^+$, circulating neutrophils (Fig. 3a). Analysis of the granule content of blood neutrophils from *MRP8*^{CRE} *Cxcr2*$^{fl/fl}$ (referred to as CXCR2$^{\Delta N}$ hereafter)[12], which have a neutrophil-specific deficiency in CXCR2, at ZT5 and ZT13, showed no differences in MPO$^+$ granule content or in side-scatter properties in blood neutrophils, compared with neutrophils from wild-type mice (Fig. 3b and Extended Data Fig. 2b). CXCR2$^{\Delta N}$ neutrophils degranulated in response to PMA and lipopolysaccharide (LPS) (Extended Data Fig. 3a,b), indicating that degranulation could be induced in these cells. We also found a loss of diurnal oscillations in granule content in blood neutrophils from *Cxcl2*$^{-/-}$ mice (Fig. 3b). Neutrophils from CXCR2$^{\Delta N}$ and *Cxcl2*$^{-/-}$ mice also showed no differences in NET formation between ZT5 and ZT13 (Fig. 3c). In chimeric mice transplanted with equal mixes of bone marrow from DsRed$^+$ wild-type and *Cxcl2*$^{-/-}$ mice, *Cxcl2*$^{-/-}$ neutrophils had a higher granule content than wild-type neutrophils analyzed at the same time (ZT5; Fig. 3d), suggesting that CXCL2 signaled in neutrophils in an autocrine fashion to control granule content.

Circadian expression of *Cxcl2* in neutrophils is controlled by the transcription factor Bmal1 (ref. [12]). *MRP8*^{CRE} *Arntl*$^{fl/fl}$ mice, which have a neutrophil-specific deletion of *Arntl* (which encodes Bmal1, referred hereafter as Bmal1$^{\Delta N}$) showed no circadian differences in MPO$^+$ granule content between ZT5 and ZT13 (Extended Data Fig. 4a) and NET formation (Extended Data Fig. 4b) in blood Ly6G$^+$ neutrophils compared to neutrophils from wild-type controls, suggesting that Bmal1 controlled the changes in the neutrophil proteome. Proteome analysis in Ly6G$^+$ neutrophils purified at ZT5 (day) or ZT13 (night) from the blood of Bmal1$^{\Delta N}$ mice (Extended Data Fig. 4c and Supplementary Table 5) indicated that Bmal1$^{\Delta N}$ neutrophils did not show circadian changes in granule proteins or in NET-associated proteins (Extended Data Fig. 4d,e). These data

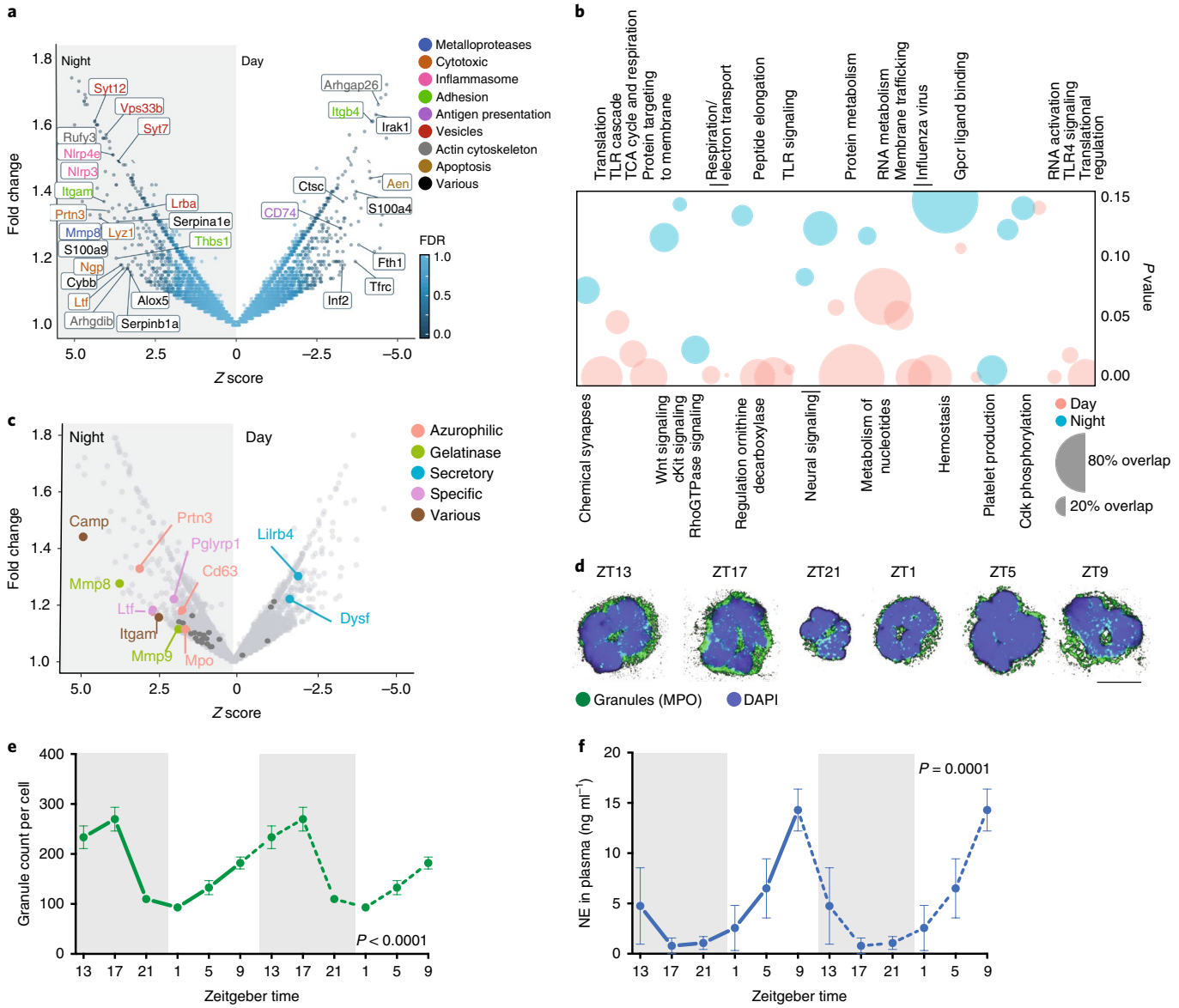

Fig. 1 | Diurnal changes in the neutrophil proteome. a, Volcano plot of the total proteome showing proteins with FDR < 0.01 (calculated as stated in the Methods from single samples of 60 million neutrophils pooled from nine mice (night) and six mice (day)). A positive *Z* score represents an increase in nighttime (fresh) over daytime (aged) neutrophils. Color represents the functional category for each protein (top right). **b**, Gene-set enrichment analysis of the proteomics data showing pathways with $P < 0.15$ enriched in aged (red) or fresh (blue) neutrophils. The size of the bubble-plot represents overlap between the query and the gene set (bottom right). Vertical lines indicate queries with multiple pathways. **c**, Volcano plot of the proteomic dataset showing granule proteins with a *Z* score >2. Colors show the granule type for each protein (top right). **d**, *Z* stack maximum projection of neutrophils stained for primary granules with MPO and counterstained with DAPI. Scale bar, 5 µm. **e**, Quantification of neutrophil granule contents during a full diurnal cycle. Curves are repeated (dashed line) to better appreciate the circadian pattern. Dark phase is shown in gray; $n = 30$ cells per time point. **f**, Neutrophil elastase (NE) activity in plasma. Curves are repeated (dashed line) to better appreciate the circadian pattern. Dark phase is shown in gray; $n = 4$ mice per time point. Data in **e** and **f** are shown as mean ± s.e.m., and circadian oscillation *P* values were determined by amplitude versus zero two-tailed *t*-test analysis (see Methods).

indicated that Bmal1 and signaling through CXCL2–CXCR2 controlled the changes in granule content and the loss in the capacity to form NETs in neutrophils.

The severity of lung injury varies during the day. To test whether the diurnal changes in the neutrophil proteome influenced the outcome of inflammatory responses in tissues, we used a model of endotoxin and antibody-induced acute lung inflammation (ALI)[15,23], which is dependent on neutrophils and NETs[24–26], and recapitulates the pulmonary injury observed in transfused patients[27]. We used ALI-prone Balb/c mice, which displayed normal diurnal variations in neutrophil number and phenotype (Extended Data Fig. 5a–c)[12]. Lungs from Balb/c mice treated to induce ALI (by intraperitoneal injection of 0.1 mg kg^{-1} LPS 24 h before intravenous injection of 0.5 mg kg^{-1} of an anti-H2d antibody) showed evidence of NETs, defined by staining for MPO, DNA and cit-H3 (Fig. 4a and Supplementary Videos 1 and 2)[24,26]. To assess the kinetics of NET formation in vivo during ALI, we performed high-speed multichannel intravital imaging of the lung microcirculation[28]. Neutrophils were identified by Ly6G staining, while NET-like structures where identified by the rapid extrusion of Sytox-green-labeled DNA from Ly6G$^+$ neutrophils, as a result of intravenous injection of the

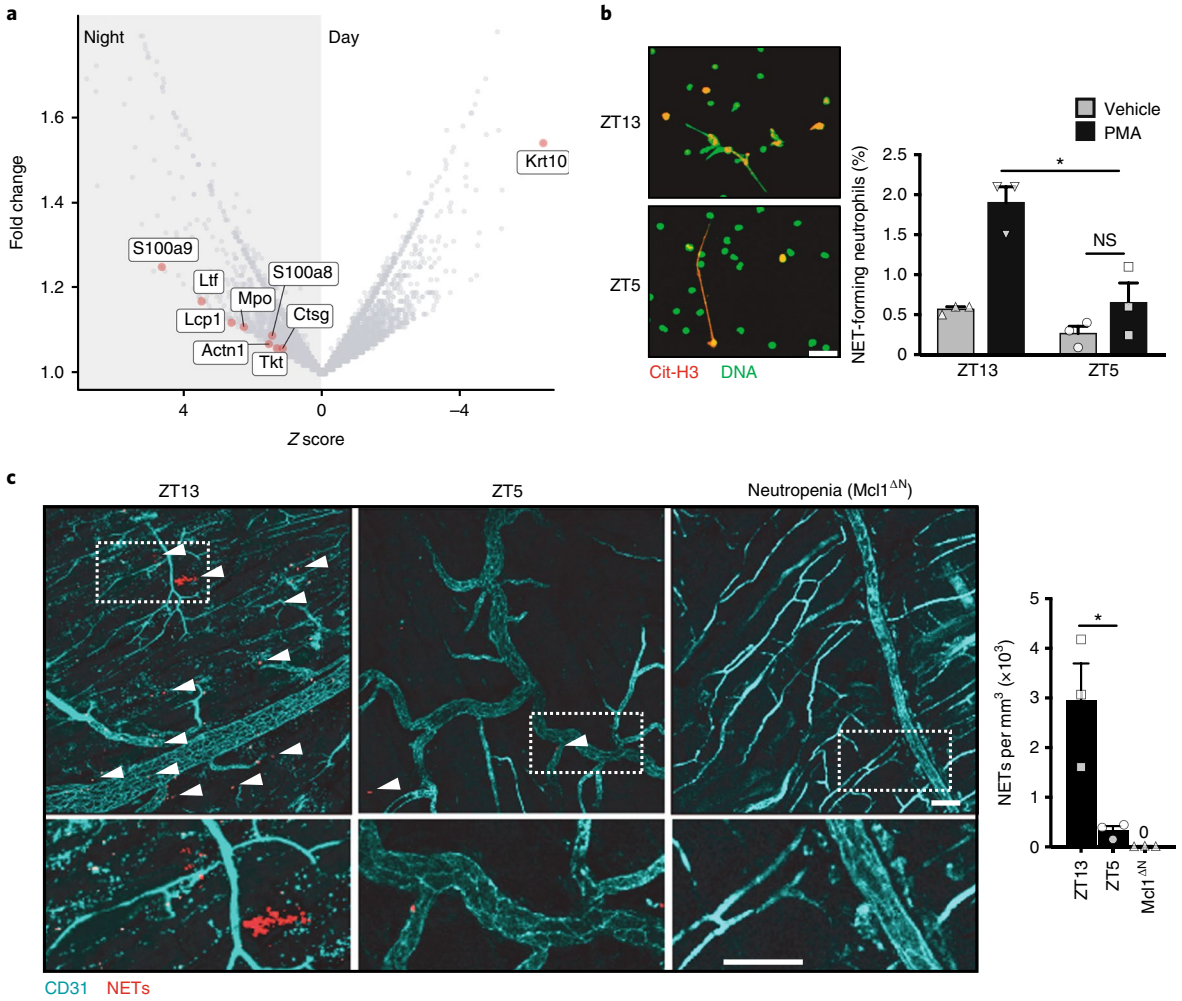

Fig. 2 | Diurnal loss of NET-forming capacity. a, Volcano plot of the neutrophil proteome showing proteins found in NETs (red dots), and enrichment of these proteins in nighttime neutrophils. **b**, Ex vivo NET-formation assay. Neutrophils sorted at ZT13 (nighttime) or ZT5 (daytime) were stimulated with PMA or vehicle to induce NETs and were stained for cit-H3 and DNA (left). Colocalization of both markers was used to quantify NET formation, as shown in the bar graph (right); $n=3$ mice per time point. **c**, Representative images (left) and quantification (right) of in vivo NET formation in the cremaster muscle subjected to ischemia/reperfusion at nighttime (ZT13) or at daytime (ZT5). Triple colocalization of MPO, DNA and cit-H3 was used to define and quantify the area of NETs (red; arrowheads). Neutropenic Mcl1$^{\Delta N}$ mice (Lyz2^{Cre};Mcl1$^{fl/fl}$ mice) were used as controls and showed no NETs. Dotted areas are shown magnified in the bottom panels; $n=3$ mice per condition. Scale bars, 50 µm. Bars show mean ± s.e.m. *$P<0.05$; NS, not significant, as determined by unpaired two-tailed *t*-test analysis.

dye 5 min before imaging (Fig. 4b and Supplementary Video 3). The Sytox-green$^+$ extrusions were inhibited by the PAD4 inhibitor chloramidine injected intravenously 1 h before induction of ALI (Fig. 4c), indicating that they represented NETs. Continuous tracking of neutrophil behavior for 40 min showed higher release of Sytox-green$^+$ extrusions at ZT13 compared with ZT5 (Fig. 4c and Supplementary Video 3). The enhanced NET production at night was detectable minutes after induction of ALI and was sustained for the rest of the experiment (Fig. 4c). In contrast, the number of Ly6G$^+$ neutrophils was similar at ZT5 and ZT13 in untreated and in chloramidine-treated mice (Extended Data Fig. 6a–c). Because platelets have been involved in neutrophil activation and NET formation during ALI[15,25], we assessed their possible involvement in the observed differences between ZT5 and ZT13. We found a sharp increase in the number of platelets in the pulmonary vessels in mice with ALI; however, their numbers were comparable at ZT5 and ZT13 (Extended Data Fig. 6b), suggesting that the number of neutrophils or platelets did not influence the diurnal changes in pulmonary NET formation.

To evaluate the effects of the diurnal changes in NET formation in the inflamed lungs, we measured the kinetics of edema formation, which is caused by infiltration of plasma in the alveolar space. Intravenous injection with Evans blue dye after ALI induction at ZT5 indicated a marked increase in pulmonary vascular permeability during ALI, compared to LPS-only treated mice (Extended Data Fig. 7a), which was specific to the lungs. We then used computerized tomography (CT) to track the in vivo dynamics of edema in mice in which we induced ALI at ZT5 (day) or at ZT13 (night). We found a rapid and sharp increase in water content of the lungs, which occurred earlier and was higher in ZT13- compared with ZT5-induced mice (Fig. 4d,e). This correlated with reduced survival of mice in which ALI was induced at ZT13 compared to those induced at ZT5 (Fig. 4f). Finally, treatment with chloramidine 1 h before induction at ZT5 protected mice from edema and death (Fig. 4e,f), indicating that the release of NETs was a primary cause of ALI. Thus, the severity of lung injury during ALI displays diurnal patterns that correlate with the granule content and the capacity of neutrophils to form NETs.

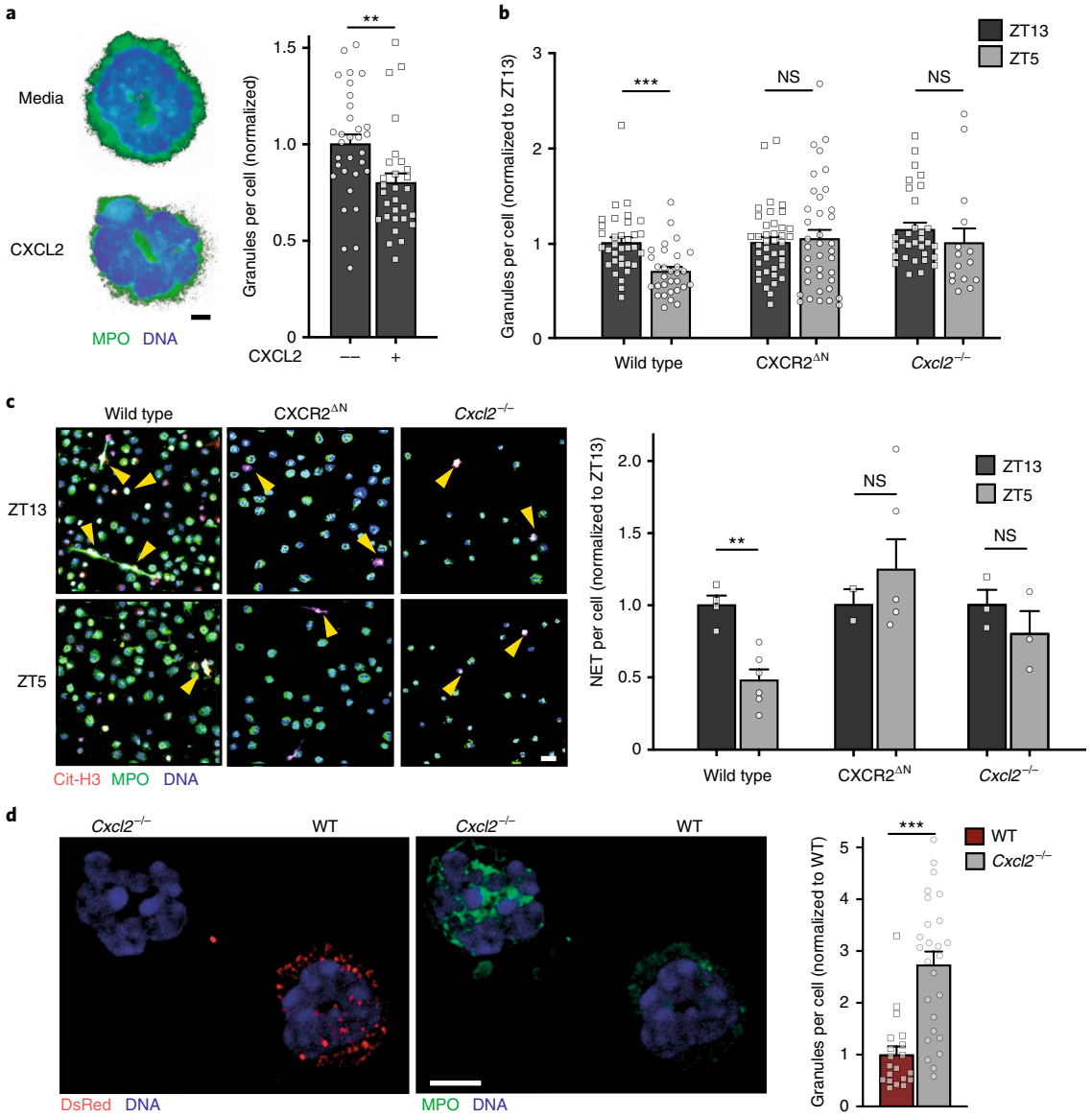

Fig. 3 | Degranulation and loss of NET-forming capacity are driven by CXCL2/CXCR2 signaling. a, Ex vivo stimulation of sorted neutrophils with CXCL2 induces degranulation (right), as quantified by confocal imaging of MPO-stained neutrophils (left); $n = 29$ (−) and 32 (+) cells. Scale bar, 2 µm. **b**, Diurnal quantification of granule content in neutrophils from WT, CXCR2$^{\Delta N}$ or *Cxcl2*$^{-/-}$ mice, showing a loss of diurnal fluctuation in CXCR2-deficient ($n = 38$ cells at ZT5 and 40 cells at ZT13) or CXCL2-deficient neutrophils ($n = 31$ cells at ZT5 and 14 cells at ZT13), compared to their WT counterparts ($n = 30$ cells at ZT5 and 34 cells at ZT13). **c**, Ex vivo NET-formation assays with sorted neutrophils stimulated with PMA or vehicle control, at nighttime (ZT13) or daytime (ZT5). NETs were quantified by triple colocalization of cit-H3, DNA and MPO in confocal micrographs (left; scale bar, 25 µm). Each mouse was normalized to its vehicle control and NET formation at ZT13 and ZT5 is compared (right). CXCL2-deficient ($n = 3$ mice per time) and CXCR2-deficient ($n = 6$ mice at ZT5 and 2 mice at ZT13) neutrophils showed loss of diurnal fluctuation in NET formation compared with WT cells ($n = 6$ mice at ZT5 and 4 mice at ZT13). **d**, CXCL2 signaling causes cell-autonomous degranulation, as shown by analysis of MPO^{+} granules in neutrophils from bone marrow chimeras reconstituted with DsRed^{+} wild-type and DsRed^{NEG} *Cxcl2*$^{-/-}$ donors; scale bar, 5 µm; $n = 3$ mice. Bars show mean ± s.e.m. $^{**}P < 0.01$; NS, not significant, as determined by paired (**a**,**d**) or unpaired (**b**,**c**) two-tailed *t*-test analysis.

Variations in the neutrophil proteome drive lung injury. To assess whether neutrophil-intrinsic variations in granule content and NET formation caused lung inflammation, we used Bmal1$^{\Delta N}$ and *MRP8*^{CRE} *Cxcr4*$^{fl/fl}$ mice, which lacked CXCR4, a negative regulator of CXCR2 signaling[12], specifically in neutrophils (hereafter CXCR4$^{\Delta N}$). Neutrophils from Bmal1$^{\Delta N}$ and CXCR4$^{\Delta N}$ mice share transcriptional and migratory properties with night and day neutrophils, respectively[12]. MPO immunofluorescence and transmission electron microscopy (TEM) imaging of blood Ly6G^{+} neutrophils purified at ZT5 revealed higher azurophilic granule content in Bmal1$^{\Delta N}$ neutrophils compared with wild-type neutrophils, and comparable with that of ZT13 wild-type neutrophils (Fig. 5a,b). In contrast, CXCR4$^{\Delta N}$ neutrophils at ZT5 had strong reductions in azurophilic granule content compared with wild-type neutrophils at any time point (Fig. 5a,b). NET formation in response to PMA was elevated in ZT5 Bmal1$^{\Delta N}$ neutrophils, and strongly reduced in CXCR4$^{\Delta N}$ neutrophils, relative to ZT5 wild-type neutrophils (Fig. 5c). Thus, variations in granule content and NET formation are driven by a neutrophil-intrinsic program.

To test whether the diurnal changes in the susceptibility to ALI were caused by changes in neutrophil granularity, we analyzed the responses of Bmal1$^{\Delta N}$ and CXCR4$^{\Delta N}$ mice to induction of ALI at

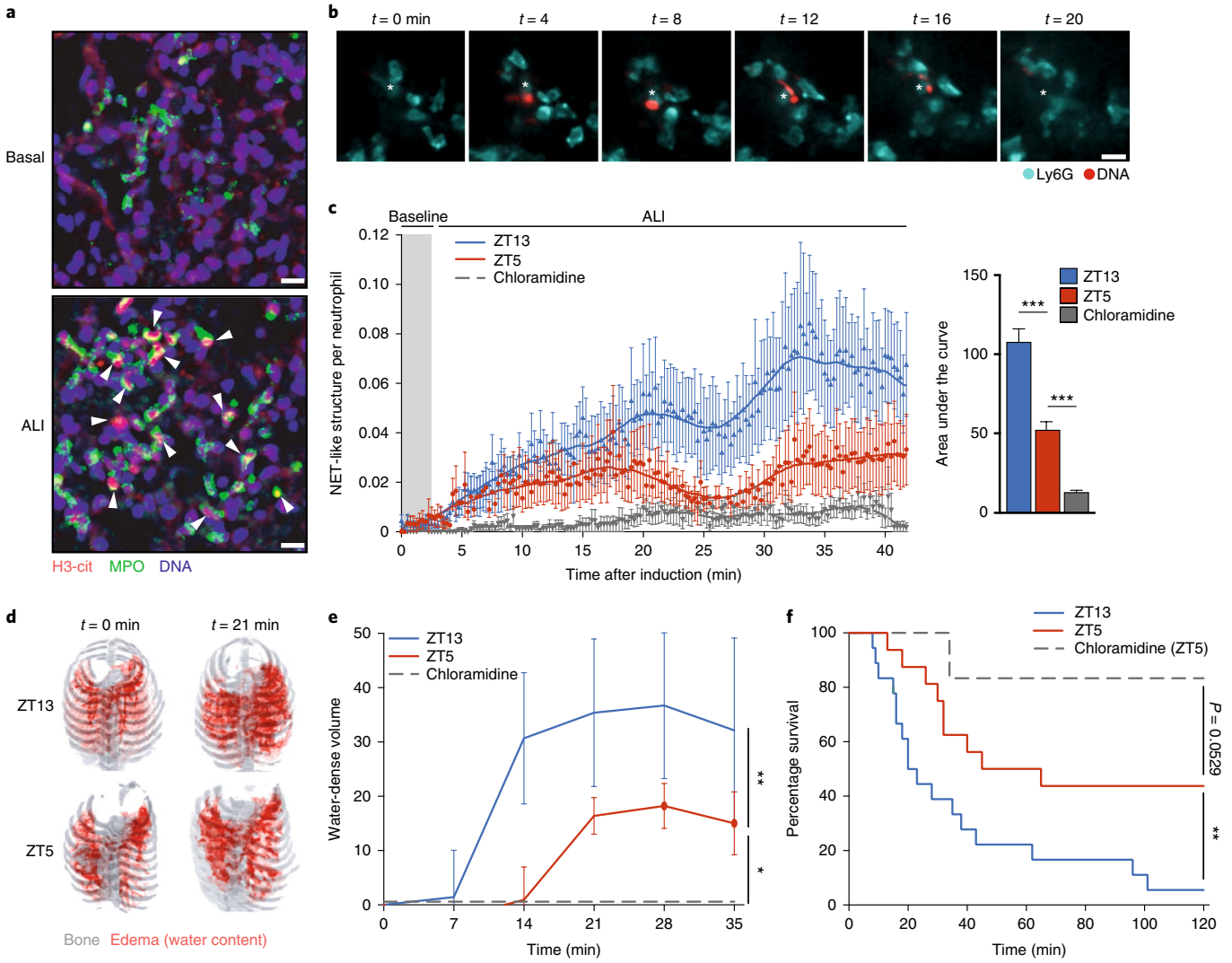

Fig. 4 | Diurnal loss of NET formation and pulmonary protection during ALI. a, Presence of NETs in lungs. Maximum projections of confocal *Z* stack series of cleared lungs from control mice (basal) or mice with antibody-induced ALI are shown. Lungs were stained against cit-H3, MPO and DNA, and some NETs are shown (arrowheads). Scale bar, 30 µm. Representative images of $n=3$ cleared lungs per condition. **b**, Time series of intravital imaging captures of NET-like structures in the lungs of ALI-induced mice. NET-like structures were defined as free DNA extruded out of Ly6G$^+$ neutrophils. Scale bar, 10 µm. See also Supplementary Video 1. **c**, Quantification of NET-like structures as shown in **b**, and normalized to the number of neutrophils in mice in which ALI was performed at nighttime (ZT13, blue line) or daytime (ZT5, red line), or in mice treated with chloramidine (at ZT5, dashed gray line). Time course (left panel) and area under the curve values (right panel); in both, $n=15$ fields from four mice per condition. Individual data points are not shown here as this graph uses a mean ± s.e.m. value for the area under the curve calculated from the data shown in the left panel. **d**, Representative images of longitudinal CT series of edema formation at 0 or 21 min after inducing ALI ZT13 or ZT5. Note the increased edema (red) at night. Background bone signal (gray) is shown for anatomical positioning. **e**, Quantification of the images in **d**. Volume of edema was increased at ZT13 (blue; $n=7$ mice) relative to ZT5 (red; $n=7$ mice). Mice treated with chloramidine are shown as a control (gray, $n=4$ mice). **f**, Survival of mice subjected to ALI at ZT13 (blue, $n=18$ mice) or ZT5 (red, $n=21$ mice), or treated with chloramidine (gray, $n=11$ mice). Data are shown as mean ± s.e.m. $^*P<0.05$; $^{**}P<0.01$; $^{***}P<0.001$, as determined by one-way ANOVA with Dunnet's multiple comparison test (**c**), two-way ANOVA (**e**) or log-rank (two-tailed Mantel–Cox) test (**f**).

ZT5. Intravital microscopy analyses showed faster and elevated NET formation in the lungs of Bmal1$^{\Delta N}$ mice compared with lungs of CXCR4$^{\Delta N}$ mice, which were similar to the differences found at ZT13 and ZT5, respectively, in wild-type mice (Fig. 5d). Intravital microscopy and flow cytometry showed similar numbers of neutrophils and platelets, as well as the number of interactions with each other, within the microvasculature of wild-type, Bmal1$^{\Delta N}$ and CXCR4$^{\Delta N}$ mice (Extended Data Fig. 6d–g), indicating an otherwise normal behavior of intravascular neutrophils in these mice. We found marked elevation in pulmonary edema and reduced survival in Bmal1$^{\Delta N}$ mice during ALI induced at ZT5 compared with CXCR4$^{\Delta N}$ mice (Fig. 5e,f and Supplementary Video 4). The protection from pathology correlated with preservation of vascular permeability in the lungs of CXCR4$^{\Delta N}$ mice after intravenous injection of Evans blue (Extended Data Fig. 7b,c). Intravital imaging in wild-type mice allowed visualization of two distinct NET-like formation events, 'flowing' NETs, in which the extruded NETs were immediately washed away by the bloodstream, and 'adherent' NETs, in which the extruded DNA remained adherent to the vasculature (Extended Data Fig. 7d and Supplementary Video 5). The frequency of adherent NETs was elevated compared with flowing NETs in Bmal1$^{\Delta N}$ mice, but not in wild-type or CXCR4$^{\Delta N}$ mice (Extended Data Fig. 7e), suggesting that the ability of neutrophils to deposit NETs onto the endothelium enhanced vascular damage in Bmal1$^{\Delta N}$ mice.

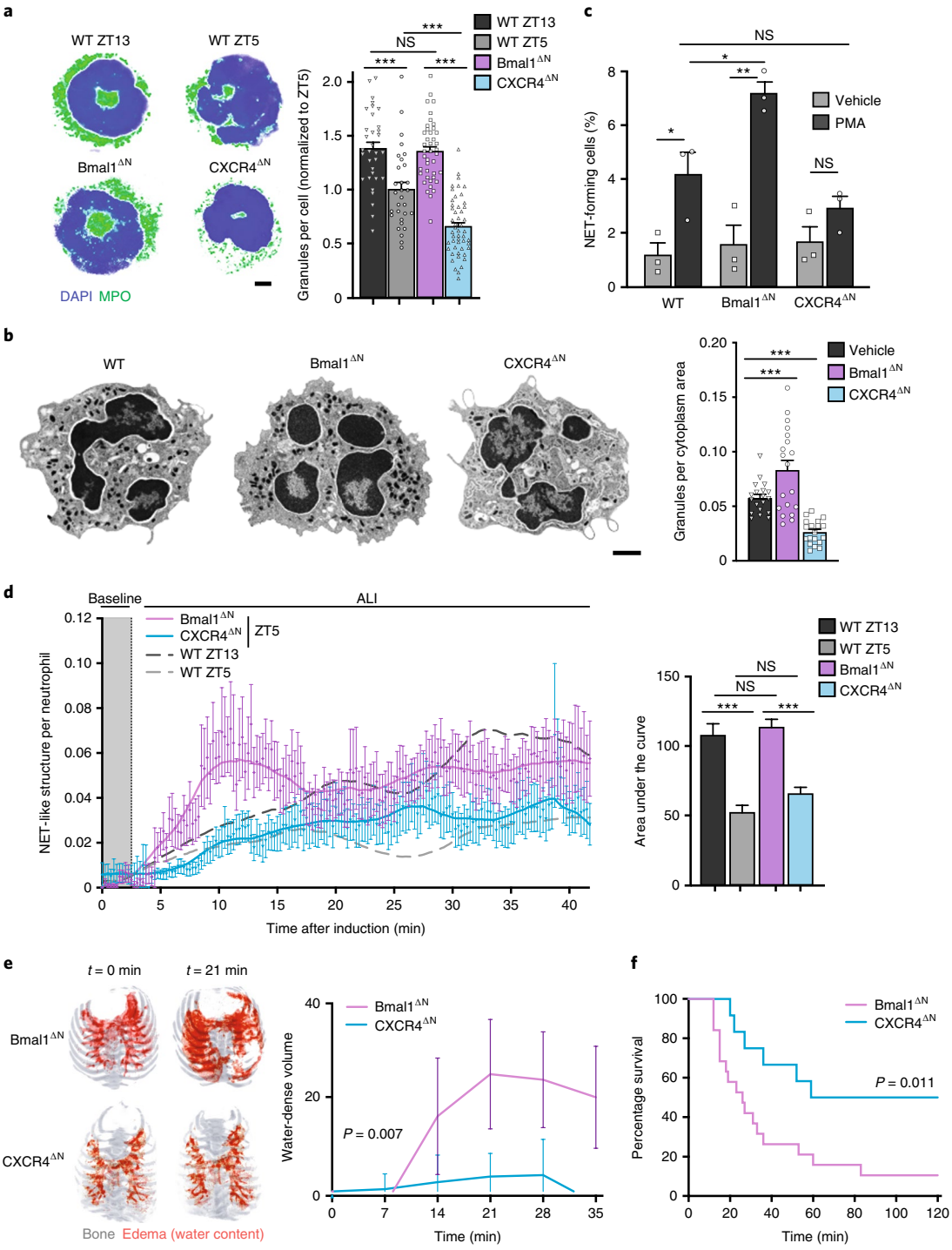

Fig. 5 | Diurnal degranulation and pulmonary protection is neutrophil intrinsic. a, Confocal micrographs (left) and quantification (right) of primary granules in neutrophils from WT mice at night (ZT13, $n=33$ cells from three mice) or daytime (ZT5, $n=30$ cells from three mice), and from mutant mice ($n=50$ cells from three CXCR4$^{\Delta N}$ mice and 41 cells from three Bmal1$^{\Delta N}$ mice, both at ZT5); scale bar, 2 µm. **b**, TEM images (left) and quantification of electrodense azurophilic granules (right) in WT and mutant mice (all at ZT5), showing increased granule content in Bmal1$^{\Delta N}$ and reduced in CXCR4$^{\Delta N}$ neutrophils compared with WT cells; $n=19$ cells from three mice each; scale bar, 1 µm. **c**, Ex vivo NET formation in sorted WT, Bmal1$^{\Delta N}$ or CXCR4$^{\Delta N}$ neutrophils stimulated with PMA or vehicle as control; $n=3$ mice per condition. **d**, Quantification of NET-like structures normalized to the number of neutrophils during ALI in Bmal1$^{\Delta N}$ (purple line) or CXCR4$^{\Delta N}$ (blue line) mice. Time course and elevations from baseline (gray area) are shown in the left panel, and the areas under the curve are shown in the right panel (individual data points are not shown here as this graph uses a mean ± s.e.m. value for the area under the curve calculated from the data shown in the left panel). Experiments were performed at ZT5. Data from wild-type mice at ZT5 (light gray, dashed) and ZT13 (dark gray, dashed) from Fig. 4c are shown for reference; $n=15$ fields from three mice for each condition. **e**, Representative images of longitudinal CT series of edema (red) in mutant mice subject to ALI (left) at ZT5, and quantification of the edema volume over time (right); $n=7$ mice per genotype. **f**, Survival curves for Bmal1$^{\Delta N}$ ($n=19$ mice) and CXCR4$^{\Delta N}$ ($n=12$ mice) mice subjected to ALI at ZT5. Data are shown as mean ± s.e.m. $^{*}P<0.05$; $^{**}P<0.01$; $^{***}P<0.001$; NS, not significant, as determined by one-way ANOVA with Dunnet's multiple comparison test (**a**–**d**), two-way ANOVA (**e**) or two-sided log-rank (Mantel–Cox) test (**f**).

Next, we tested the causal relationship between the diurnal proteome changes in neutrophils and the diurnal susceptibility to inflammation in the Bmal1$^{\Delta N}$ mice. Neutrophils from Bmal1$^{\Delta N}$ mice had a constitutively high MPO^{+} granule content and NET-forming capacity (Extended Data Fig. 4a,b) and reduced survival during ALI at both ZT5 or ZT13 (Extended Data Fig. 8a). CXCR4$^{\Delta N}$ neutrophils, in turn, had a similar loss in circadian granule content and NET formation (Extended Data Fig. 8b,c) and higher survival during ALI at both ZT5 or ZT13 (Extended Data Fig. 8a). Of note, the number of circulating neutrophils in Bmal1$^{\Delta N}$ mice oscillated during the day, similar to wild-type mice (Extended Data Fig. 8d), whereas CXCR4$^{\Delta N}$ mice display constitutively high neutrophil counts[12], indicating that the granule content, but not the number of neutrophils, was associated with the severity of pulmonary inflammation. These observations indicated that impaired diurnal changes in the proteome and the granule content in neutrophils were related to the magnitude of inflammation.

Human neutrophils undergo proteome disarming. Clinical manifestations of inflammation display circadian oscillations in humans, and are associated with time-of-day variations in both the incidence and the severity of cardiovascular disease[29–31]. We tested whether neutrophil 'disarming' in humans could underlie the circadian changes in vascular inflammation. We measured neutrophil counts in blood and performed proteomic analysis, granule content and NET-formation assays in neutrophils isolated at 8:00, 14:00 and 17:00 (Extended Data Fig. 9a), when diurnal patterns in neutrophil number and phenotype are prominent in humans[12], from ten healthy volunteers. Human neutrophils display a night-like phenotype (similar to murine ZT13) early in the morning, and progress toward a day-like phenotype (similar to murine ZT5) over the next 4–8 h (ref. [12]). In our cohort, neutrophil counts increased over time and peaked at 14:00–19:00 (Fig. 6a), while the granularity of neutrophils, indicated by the side scatter by flow cytometry, decreased from 8:00 to 19:00 (Fig. 6b). Direct examination of granules in human neutrophils stained for MPO (Fig. 6c,d), as well as by TEM imaging (Fig. 6e), indicated a diurnal reduction in granule content, which peaked at 8:00 and showed a trough at 14:00.

Proteomic analyses of neutrophils isolated in density gradients at 8:00 and 14:00 from the blood of five healthy volunteers (Supplementary Table 6) indicated that, from a total of 1,918 proteins detected, around 9.7% were differentially enriched between 8:00 and 14:00 ($P < 0.05$; Fig. 6f). Gene ontology analyses revealed that the differentially detected proteins were in pathways related to vesicle-mediated transport, secretion, exocytosis or degranulation (Extended Data Fig. 9b and Supplementary Table 7), consistent with a loss of granule content in human neutrophils over time. Many of the individual proteins identified in the mouse analyses were not detected or did not show diurnal changes in the human samples (not shown), probably indicating a high variability among humans compared with co-housed and strain-matched mice. However, numerous granule proteins, such as MPO, MMP9 or LTF, were more abundant at 8:00 than at 14:00 in human neutrophils (Fig. 6g). Similar to mouse neutrophils, there was a poor correlation between transcript and protein amounts in human neutrophils (Extended Data Fig. 9c), suggesting that the proteomic changes were largely independent of transcriptional regulation. Ex vivo assays of human neutrophils purified using density gradients and treated with vehicle or PMA indicated a marked reduction in NET-forming capacity between 8:00 and 14:00 (Fig. 6h,i), corresponding with more NET-related proteins at 8:00 compared with 14:00 (Extended Data Fig. 9d). These observations suggested that diurnal degranulation also occurred in circulating human neutrophils.

Finally, we tested whether the changes in proteome, granule content and NET-forming activity in human neutrophils were associated with variations in the susceptibility to develop inflammation and/or its severity. We focused on an existing cohort of 5,334 patients with community-acquired pneumonia, who are at risk of developing acute respiratory distress syndrome (ARDS)[32]. Retrospective analysis of the human cohort indicated that, among the patients hospitalized with community-acquired pneumonia, 125 (2.3%) developed ARDS. Assessment of the temporal patterns of disease onset and severity (using the pneumonia severity index), by plotting the times of admission against the pneumonia index and death in this subset of patients, revealed consistent diurnal oscillations, with a peak around 9:00 and a trough at 17:00–19:00 for both parameters (Fig. 6j). These observations indicate that proteomic disarming occurs in human neutrophils and may influence the incidence and severity of inflammation (Extended Data Fig. 10 and Supplementary Video 6).

Discussion

Here, we describe the existence of a cell-intrinsic program in neutrophils that induced the progressive loss of granule proteins involved in inflammation and the formation of NETs, and provided a previously unrecognized layer of protection against the toxic activity of these leukocytes. The phenomenon of proteome disarming described here shares key features with the process of neutrophil 'aging'[12], in terms of reliance on CXCR2 signaling, regulation by Bmal1 and CXCR4 in a cell-intrinsic manner and similar temporal patterns (that is, peak at noon). This suggested that neutrophil aging and disarming might represent distinct manifestations of a core circadian program in neutrophils that allows anticipation of potential threats[12], but also protects from excessive inflammation, vascular damage and death.

Beyond regulating the magnitude of inflammation, changes in the neutrophil proteome displayed temporal oscillations that aligned neutrophil activity with circadian cycles. The circadian transcriptional regulation of migration-associated genes by Bmal1 controls the migratory properties of neutrophils, and allows the infiltration of naïve tissues in anticipation of potential infections[12]. In addition to these transcription-mediated mechanisms, we uncovered here that the neutrophil proteome is also subject to circadian regulation, which blunts the ability of neutrophils to release toxic mediators and to produce NETs. This level of immune regulation may be particularly relevant for granulocytes, a group of innate immune cells that synthesize and store the majority of their early-response mediators inside dedicated organelles. Because the formation of granules and their content occurs as neutrophils differentiate in the bone marrow[7,33], it is unlikely that changes of the granule proteome that occur in the circulation are transcriptionally regulated, as illustrated by the poor correlation between the proteome and the transcriptome in these cells. Our data, however, suggested a model in which upstream control of transcription of *Cxcl2* by Bmal1 (ref. [12]) allowed indirect regulation of the neutrophil proteome by the canonical circadian machinery. Conceptually, the temporal nature of this process in blood aligns with the evolutionary value of circadian oscillations in segregating mutually antagonistic processes, in this case potent antimicrobial responses and protection of the host against immune-mediated damage.

The circadian patterns in the granule content and elastase activity in plasma suggested the progressive discharge of granules while in the circulation, such that neutrophils that migrate into tissues during the day[10] would have lost part of their antimicrobial arsenal, and would be, as such, less likely to elicit organ damage, as shown in the mouse model of ALI. Because neutrophil proteases are also important for the activation of many biological mediators, including cytokines, chemokines, growth factors and adhesion and pattern-recognition receptors[34,35], and even modulate signaling cascades in other cells[36,37], the programmed proteome changes reported here may have pleiotropic consequences in physiology. For instance, they predict that neutrophils that are newly released from the bone marrow in conditions of stress, such as obesity or cancer[38,39], may be

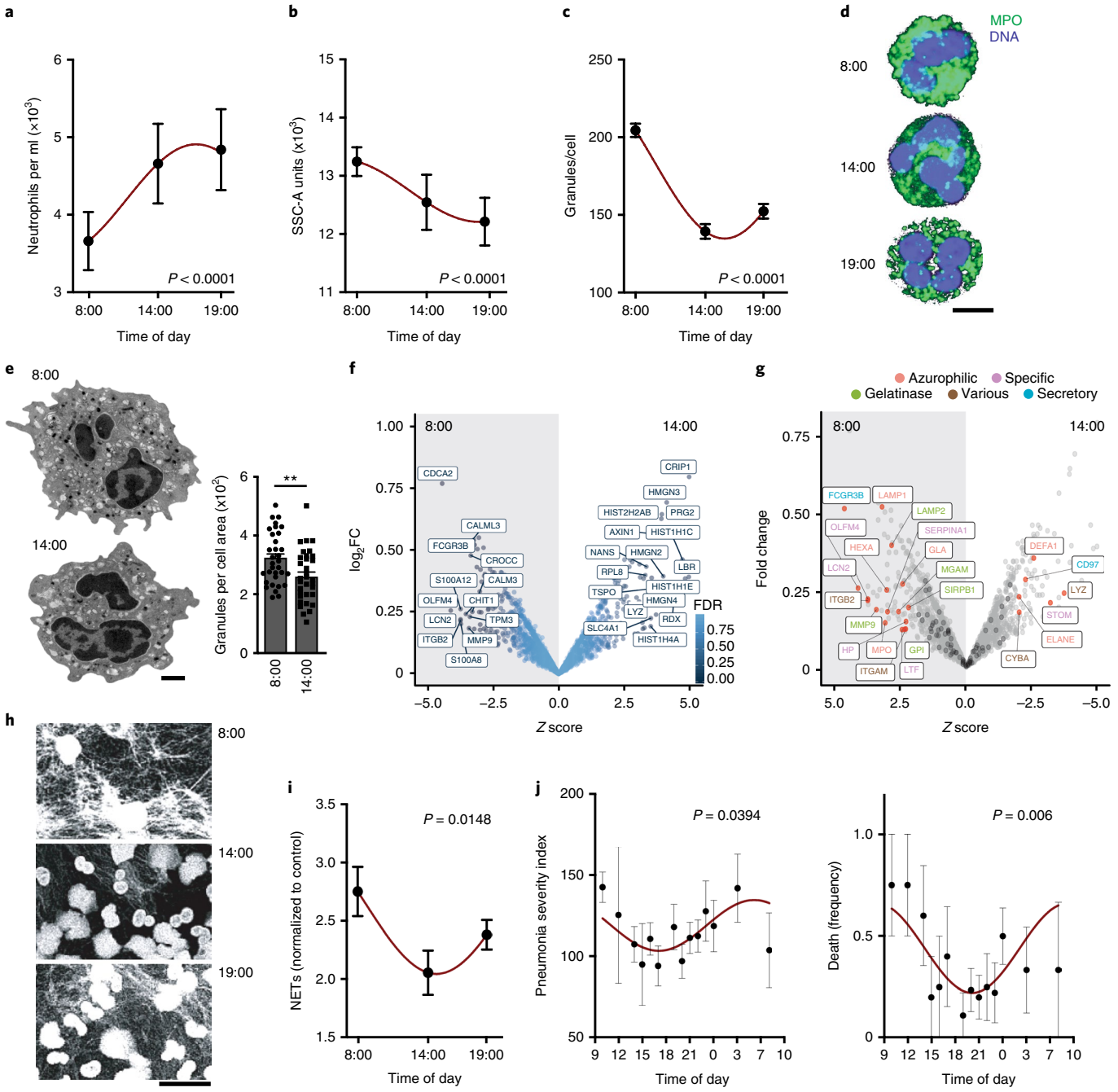

Fig. 6 | Evidence for neutrophil disarming and pulmonary protection in humans. a, Blood neutrophil counts in human volunteers at the different time points; $n=10$ human volunteers per time point. **b**, Light-scattering (SSC-A) values for human neutrophils at different times, as measured by flow cytometry; $n=10$ human volunteers. **c**, Quantification of primary granules from confocal images of human neutrophils from images in **d**; $n=150$ cells from ten volunteers per time point. **d**, Representative images of granule content of human neutrophils, quantified in **c**. **e**, Transmission electron micrographs (left) of human neutrophils in the morning (8:00) and early afternoon (14:00), and quantification (right) showing reduced numbers of electrodense primary granules; $n=33$ cells from three human volunteers per time point. **f**, Volcano plot of the human neutrophil proteome analyzed at 8:00 and 14:00, showing proteins with $P<0.001$ (see Methods for human TMT proteomics). A negative Z score represents higher values at 8:00 over 14:00 neutrophils; $n=5$ per time point. **g**, Volcano plot of granule proteins in the human neutrophil proteome, showing higher content in granule proteins (color-coded) at 8:00 compared with 14:00; $n=5$ samples from healthy volunteers. Red dots and labels show differentially expressed proteins with $P<0.05$, and black dots show all granule proteins. Label color indicates the granule type in which the protein is normally found (top right). **h**,**i**, Representative confocal images (**h**) and quantification (**i**) of ex vivo NET formation by human neutrophils stimulated with PMA or vehicle at the indicated time points; $n=10$ volunteers per time point. **j**, ARDS severity shown as the pneumonia severity index (left) and intrahospital deaths (right) of patients entering the intensive care unit at different times of the day; $n=125$ patients. Data are shown as mean ± s.e.m. $^{**}P<0.01$, as determined by unpaired two-tailed t-test analysis (**f**). P values for the circadian plots were calculated by the amplitude versus zero two-tailed t-test analysis (**a**–**c**,**g**,**i**). Maroon line in **a**–**c**, **g** and **i** shows the nonlinear COSINOR fit of the data.

better suited to regulate physiological aspects of target organs than the aged neutrophils that enter the tissues at the end of their life cycle and have lost part of their cargo.

Our observations shed light into the particular susceptibility of the lungs to diurnal inflammation. Large numbers of neutrophils accumulate within the pulmonary microcirculation in mice, rabbits and nonhuman primates after stimulation or in the steady state[10,18,40], and the lungs can provide a niche for effective antimicrobial responses[41]. The homeostatic accumulation of neutrophils in the lungs at the end of the light cycle in mice[10] would predict higher susceptibility to inflammatory stimuli at this time. However, we found that neutrophils recovered from naïve lungs had reduced granularity, and that mutant mice with constitutive low levels of granules in neutrophils displayed permanent protection from ALI, suggesting a dominant contribution of the disarming process in tissue protection.

It has long been recognized that multiple inflammatory processes in humans display circadian periodicity[42], and experimental models and retrospective studies have corroborated that not only the onset of inflammation, but also the severity of the inflammatory events manifest diurnal oscillations[31]. These events are often caused by neutrophil activation and by thrombosis, which in turn can be exacerbated in the presence of neutrophils or NETs[15,25,43,44]. Thus, our current findings in the context of ALI may extend to other inflammatory and thrombotic conditions affecting multiple organs, and suggest that interventions aimed at inducing controlled degranulation may effectively 'disarm' neutrophils and protect organs from catastrophic inflammation.

Online content

Any methods, additional references, Nature Research reporting summaries, source data, extended data, supplementary information, acknowledgements, peer review information; details of author contributions and competing interests; and statements of data and code availability are available at https://doi.org/10.1038/s41590-019-0571-2.

Received: 15 April 2019; Accepted: 3 December 2019;
Published online: 13 January 2020

References

1. Cowland, J. B. & Borregaard, N. Granulopoiesis and granules of human neutrophils. *Immunol. Rev.* **273**, 11–28 (2016).
2. Ley, K. et al. Neutrophils: new insights and open questions. *Sci. Immunol.* **3**, eaat4579 (2018).
3. Borregaard, N., Sørensen, O. E. & Theilgaard-Mönch, K. Neutrophil granules: a library of innate immunity proteins. *Trends Immunol.* **28**, 340–345 (2007).
4. Rørvig, S., Østergaard, O., Heegaard, N. H. & Borregaard, N. Proteome profiling of human neutrophil granule subsets, secretory vesicles, and cell membrane: correlation with transcriptome profiling of neutrophil precursors. *J. Leukoc. Biol.* **94**, 711–721 (2013).
5. Borregaard, N. Neutrophils, from marrow to microbes. *Immunity* **33**, 657–670 (2010).
6. Le Cabec, V., Cowland, J. B., Calafat, J. & Borregaard, N. Targeting of proteins to granule subsets is determined by timing and not by sorting: the specific granule protein NGAL is localized to azurophil granules when expressed in HL-60 cells. *Proc. Natl Acad. Sci. USA* **93**, 6454–6457 (1996).
7. Evrard, M. et al. Developmental analysis of bone marrow neutrophils reveals populations specialized in expansion, trafficking, and effector functions. *Immunity* **48**, 364–379.e8 (2018).
8. Grassi, L. et al. Dynamics of transcription regulation in human bone marrow myeloid differentiation to mature blood neutrophils. *Cell Rep.* **24**, 2784–2794 (2018).
9. Tak, T., Tesselaar, K., Pillay, J., Borghans, J. A. & Koenderman, L. What's your age again? Determination of human neutrophil half-lives revisited. *J. Leukoc. Biol.* **94**, 595–601 (2013).
10. Casanova-Acebes, M. et al. Neutrophils instruct homeostatic and pathological states in naive tissues. *J. Exp. Med.* **215**, 2778–2795 (2018).
11. He, W. et al. Circadian expression of migratory factors establishes lineage-specific signatures that guide the homing of leukocyte subsets to tissues. *Immunity* **49**, 1175–1190.e7 (2018).
12. Adrover, J. M. et al. A neutrophil timer coordinates immune defense and vascular protection. *Immunity* **51**, 966–967 (2019).
13. Grommes, J. & Soehnlein, O. Contribution of neutrophils to acute lung injury. *Mol. Med.* **17**, 293–307 (2011).
14. Looney, M. R., Su, X., Van Ziffle, J. A., Lowell, C. A. & Matthay, M. A. Neutrophils and their Fcγ receptors are essential in a mouse model of transfusion-related acute lung injury. *J. Clin. Investig.* **116**, 1615–1623 (2006).
15. Sreeramkumar, V. et al. Neutrophils scan for activated platelets to initiate inflammation. *Science* **346**, 1234–1238 (2014).
16. Matthay, M. A. & Zemans, R. L. The acute respiratory distress syndrome: pathogenesis and treatment. *Ann. Rev. Pathol.* **6**, 147–163 (2011).
17. Casanova-Acebes, M. et al. Rhythmic modulation of the hematopoietic niche through neutrophil clearance. *Cell* **153**, 1025–1035 (2013).
18. Devi, S. et al. Neutrophil mobilization via plerixafor-mediated CXCR4 inhibition arises from lung demargination and blockade of neutrophil homing to the bone marrow. *J. Exp. Med.* **210**, 2321–2336 (2013).
19. Zhang, D. et al. Neutrophil ageing is regulated by the microbiome. *Nature* **525**, 528–532 (2015).
20. Papayannopoulos, V., Metzler, K. D., Hakkim, A. & Zychlinsky, A. Neutrophil elastase and myeloperoxidase regulate the formation of neutrophil extracellular traps. *J. Cell Biol.* **191**, 677–691 (2010).
21. Urban, C. F. et al. Neutrophil extracellular traps contain calprotectin, a cytosolic protein complex involved in host defense against *Candida albicans*. *PLoS Pathog.* **5**, e1000639 (2009).
22. Csepregi, J. Z. et al. Myeloid-specific deletion of Mcl-1 yields severely neutropenic mice that survive and breed in homozygous form. *J. Immunol.* **201**, 3793–3803 (2018).
23. Looney, M. R. et al. Platelet depletion and aspirin treatment protect mice in a two-event model of transfusion-related acute lung injury. *J. Clin. Investig.* **119**, 3450–3461 (2009).
24. Caudrillier, A. et al. Platelets induce neutrophil extracellular traps in transfusion-related acute lung injury. *J. Clin. Investig.* **122**, 2661–2671 (2012).
25. Hidalgo, A. et al. Heterotypic interactions enabled by polarized neutrophil microdomains mediate thromboinflammatory injury. *Nat. Med.* **15**, 384–391 (2009).
26. Thomas, G. M. et al. Extracellular DNA traps are associated with the pathogenesis of TRALI in humans and mice. *Blood* **119**, 6335–6343 (2012).
27. Looney, M. R., Gilliss, B. M. & Matthay, M. A. Pathophysiology of transfusion-related acute lung injury. *Curr. Opin. Hematol.* **17**, 418–423 (2010).
28. Looney, M. R. et al. Stabilized imaging of immune surveillance in the mouse lung. *Nat. Methods* **8**, 91–96 (2011).
29. Muller, J. E. et al. Circadian variation in the frequency of onset of acute myocardial infarction. *N. Engl. J. Med.* **313**, 1315–1322 (1985).
30. Scheiermann, C., Kunisaki, Y. & Frenette, P. S. Circadian control of the immune system. *Nat. Rev. Immunol.* **13**, 190–198 (2013).
31. Suarez-Barrientos, A. et al. Circadian variations of infarct size in acute myocardial infarction. *Heart* **97**, 970–976 (2011).
32. Cilloniz, C. et al. Acute respiratory distress syndrome in mechanically ventilated patients with community-acquired pneumonia. *Eur. Respir. J.* **51**, 1702215 (2018).
33. Faurschou, M. & Borregaard, N. Neutrophil granules and secretory vesicles in inflammation. *Microbes Infect.* **5**, 1317–1327 (2003).
34. Meyer-Hoffert, U. Neutrophil-derived serine proteases modulate innate immune responses. *Front. Biosci. (Landmark Ed.)* **14**, 3409–3418 (2009).
35. Pham, C. T. Neutrophil serine proteases: specific regulators of inflammation. *Nat. Rev. Immunol.* **6**, 541–550 (2006).
36. Houghton, A. M. et al. Neutrophil elastase-mediated degradation of IRS-1 accelerates lung tumor growth. *Nat. Med.* **16**, 219–223 (2010).
37. Talukdar, S. et al. Neutrophils mediate insulin resistance in mice fed a high-fat diet through secreted elastase. *Nat. Med.* **18**, 1407–1412 (2012).
38. Coffelt, S. B. et al. IL-17-producing γδ T cells and neutrophils conspire to promote breast cancer metastasis. *Nature* **522**, 345–348 (2015).
39. Quail, D. F. et al. Obesity alters the lung myeloid cell landscape to enhance breast cancer metastasis through IL5 and GM-CSF. *Nat. Cell. Biol.* **19**, 974–987 (2017).
40. Doerschuk, C. M. The role of CD18-mediated adhesion in neutrophil sequestration induced by infusion of activated plasma in rabbits. *Am. J. Respir. Cell Mol. Biol.* **7**, 140–148 (1992).
41. Yipp, B. G. et al. The lung is a host defense niche for immediate neutrophil-mediated vascular protection. *Sci. Immunol.* **2**, eaam8929 (2017).
42. Muller, J. E. & Tofler, G. H. Circadian variation and cardiovascular disease. *N. Engl. J. Med.* **325**, 1038–1039 (1991).
43. Engelmann, B. & Massberg, S. Thrombosis as an intravascular effector of innate immunity. *Nat. Rev. Immunol.* **13**, 34–45 (2013).
44. Jimenez-Alcazar, M. et al. Host DNases prevent vascular occlusion by neutrophil extracellular traps. *Science* **358**, 1202–1206 (2017).